MCB
Journals.ASM.org

Thioesterase Superfamily Member 2 (Them2) and Phosphatidylcholine Transfer Protein (PC-TP) Interact To Promote Fatty Acid Oxidation and Control Glucose Utilization

Yuki Kawano,[a] Baran A. Ersoy,[a] Yingxia Li,[a] Shin Nishiumi,[b] Masaru Yoshida,[b,c,d] David E. Cohen[a]

Department of Medicine, Division of Gastroenterology, Brigham and Women's Hospital, Harvard Medical School, Boston, Massachusetts, USA[a]; Department of Internal Medicine, Division of Gastroenterology, Kobe University Graduate School of Medicine, Kobe, Japan[b]; Department of Internal Medicine related, Division of Metabolomics Research, Kobe University Graduate School of Medicine, Kobe, Japan[c]; Integrated Center for Mass Spectrometry, Kobe University Graduate School of Medicine, Kobe, Japan[d]

Thioesterase superfamily member 2 (Them2) is a mitochondrion-associated long-chain fatty acyl coenzyme A (CoA) thioesterase that is highly expressed in the liver and oxidative tissues. Them2 activity *in vitro* is increased when it interacts with phosphatidylcholine transfer protein (PC-TP), a cytosolic lipid binding protein. *Them2*$^{-/-}$ and *Pctp*$^{-/-}$ mice exhibit enhanced hepatic insulin sensitivity and increased adaptive thermogenesis, and *Them2*$^{-/-}$ mice are also resistant to diet-induced hepatic steatosis. Although we showed previously that a Them2–PC-TP complex suppresses insulin signaling, the enzymatic activity of Them2 suggests additional direct involvement in regulating hepatic nutrient homeostasis. Here we used cultured primary hepatocytes to elucidate biochemical and cellular mechanisms by which Them2 and PC-TP regulate lipid and glucose metabolism. Under conditions simulating fasting, *Them2*$^{-/-}$ and *Pctp*$^{-/-}$ hepatocytes each exhibited decreased rates of fatty acid oxidation and gluconeogenesis. In results indicative of Them2-dependent regulation by PC-TP, chemical inhibition of PC-TP failed to reproduce these changes in *Them2*$^{-/-}$ hepatocytes. In contrast, rates of glucose oxidation and lipogenesis in the presence of high glucose concentrations were decreased only in *Them2*$^{-/-}$ hepatocytes. These findings reveal a primary role for Them2 in promoting mitochondrial oxidation of fatty acids and glucose in the liver.

Thioesterase superfamily member 2 (Them2), a member of the acyl coenzyme A (CoA) thioesterase (Acot) family, catalyzes the hydrolysis of long-chain fatty acyl-CoA esters to free fatty acids plus CoA (1, 2). Them2 is enriched in liver and oxidative tissues, including brown adipose (3–5). Mice lacking Them2 (*Them2*$^{-/-}$ mice) exhibit increases in hepatic insulin sensitivity and adaptive thermogenesis in brown adipose tissue, and they are resistant to high-fat-diet-induced hepatic steatosis (6, 7).

We originally identified Them2 as a phosphatidylcholine transfer protein (PC-TP; also called StarD2)-interacting protein (3). PC-TP is a lipid binding protein with high specificity for phosphatidylcholines (3, 8). Using purified recombinant proteins, we have demonstrated that the fatty acyl-CoA thioesterase activity of Them2 is increased upon its interaction with PC-TP (1, 3). Like Them2, PC-TP is enriched in liver and oxidative tissues (3, 4), and mice lacking PC-TP (*Pctp*$^{-/-}$ mice) also exhibit increased hepatic insulin sensitivity and adaptive thermogenesis (4, 6, 7, 9).

The observed increases in hepatic insulin sensitivity in *Them2*$^{-/-}$ and *Pctp*$^{-/-}$ mice may be explained, at least in part, by our recent observation that a Them2–PC-TP complex suppresses insulin signaling by reducing the activation of both insulin receptor substrate 2 (IRS2) and mammalian target of rapamycin (mTOR) (10). However, we have also shown that Them2 expression and PC-TP expression are both under the transcriptional control of peroxisome proliferator-activated receptor α (PPARα) (1, 11), suggesting that Them2 and PC-TP may participate directly in fatty acid metabolism (12), particularly under fasting conditions, which favor fatty acid oxidation (13).

Based on observations that Them2 is localized mainly to mitochondria and that PC-TP is abundant in the cytosol (1), we have proposed that the two proteins may interact at the outer mitochondrial membrane (12) and could thereby regulate fatty acid oxidation. To test this hypothesis, we used primary hepatocytes cultured from *Them2*$^{-/-}$ and *Pctp*$^{-/-}$ mice, which allowed us to examine cellular biochemistry in isolation from the influence of *in vivo* hormonal and metabolic factors. Genetic ablation of Them2 reduced hepatic tricarboxylic acid (TCA) cycle activity. Depending on substrate availability, this resulted in decreased conversion of gluconeogenic substrates into glucose and of glucose into lipids. The absence or chemical inhibition of PC-TP suppressed Them2-dependent gluconeogenesis. However, potentially owing to dissociation of the Them2–PC-TP interaction during the fed state, PC-TP ablation did not affect rates of lipogenesis. These findings provide new insights into the molecular regulation of nutrient homeostasis within the liver.

MATERIALS AND METHODS

Animals. Male *Them2*$^{-/-}$ and *Pctp*$^{-/-}$ mice and their respective controls were as described previously (6, 9). Male FVB/NJ mice were obtained from The Jackson Laboratory. Mice were housed in a pathogen-free barrier facility under controlled lighting (12-h light/dark cycle) and were fed a standard rodent diet with free access to drinking water. The ages of mice ranged from 6 to 15 weeks, and they were matched to within 2 weeks of age

Received 5 December 2013 **Returned for modification** 22 December 2013
Accepted 8 April 2014
Published ahead of print 14 April 2014
Address correspondence to David E. Cohen, dcohen@partners.org.

doi:10.1128/MCB.01601-13

for individual experiments. All animal procedures were approved by the institutional committee of the Harvard Medical School.

Primary hepatocyte isolation. Hepatocytes were isolated by a 2-step perfusion procedure (9). Surgeries were commenced between 10 a.m. and 12 p.m., following anesthesia with 100 mg of ketamine/kg of body weight (bw) and 10 mg of xylazine/kg bw, plus 3 mg of acepromazine/kg bw. The liver was perfused *in situ* through the inferior vena cava with 20 ml of prewarmed liver perfusion medium (Invitrogen) followed by 40 ml of liver digestion medium (Invitrogen). The liver was then placed in ice-cold hepatocyte wash medium (Invitrogen), and the capsule of the liver was then gently disrupted in order to release the hepatocytes. The cell suspension was filtered with a 70-μm cell strainer (Becton, Dickinson), and cells were washed once (30 × *g*, 4 min, 4°C). Dead cells were removed using Percoll solution (Sigma-Aldrich) as described previously (14) with minor modifications. Briefly, cells in 50-ml conical tubes were resuspended in 25 ml hepatocyte wash medium and were then layered onto 20 ml Percoll solution consisting of 18 ml Percoll plus 2 ml of 10× Hanks' balanced salt solution (HBSS; Sigma-Aldrich). Cells were mixed with Percoll solution by inverting five times and were then pelleted by centrifugation at 150 × *g* for 10 min at 4°C. Following a second wash, cells were pelleted, resuspended in incubation medium, and seeded on plates as specified below. In selected experiments, adenoviral vectors were utilized to express Them2, PC-TP, or green fluorescent protein (GFP) in primary hepatocytes. A recombinant mouse adenovirus (Ad) carrying Them2 driven by the cytomegalovirus (CMV) promoter (Ad-CMV-Them2) was constructed by standard techniques utilizing the open reading frame of a mouse Them2 cDNA (ViraQuest). The recombinant mouse PC-TP adenovirus (Ad-CMV-PC-TP) used has been described previously (4). A recombinant adenovirus expressing GFP (Ad-CMV-GFP; ViraQuest) was used as a control. For adenovirus infection, primary hepatocytes were seeded on 6-well Primaria plates (Becton, Dickinson) at a density of 5×10^5 cells/well. Cells were allowed to adhere to the plates for 3 h, after which the culture medium was replaced by 1 ml of fresh serum-free medium containing adenovirus. After 2 h, the adenovirus solution was removed, and serum-free medium was added to each well. Cells were then incubated for as long as 40 h prior to harvesting.

Fatty acid oxidation. Rates of fatty acid oxidation were determined according to the conversion of [1-^{14}C]palmitate (55 mCi/mmol; American Radiolabeled Chemicals) into ^{14}C-labeled acid-soluble metabolites (ASM) and CO_2 (15). Isolated hepatocytes were seeded on type I collagen-coated 6-well plates with Williams' medium E (Invitrogen) containing 10% fetal bovine serum (FBS) and 1% penicillin-streptomycin. After the cells were allowed to attach overnight, they were incubated for 6 h in 2 ml of fresh serum-free Williams' medium E supplemented with 1 mM carnitine (Sigma-Aldrich) and 0.25 μCi [1-^{14}C]palmitate/ml plus 200 μM palmitate (Sigma-Aldrich) conjugated with fatty acid-free bovine serum albumin (BSA; Sigma-Aldrich). The cultured medium was then transferred to 15-ml conical tubes and was mixed with 200 μl of 70% perchloric acid (Fisher Scientific). During 1 h of incubation at room temperature on a horizontal shaker, CO_2 was trapped in the filter paper soaked with 2 N NaOH that was placed inside the caps of the conical tubes. The acidified medium was incubated overnight at 4°C and was then centrifuged (14,000 rpm, 20 min, 4°C). To quantify ^{14}C-labeled CO_2 and ASM, respectively, the filter paper and supernatant were each dissolved in Ecoscint H (National Diagnostics) and were counted with a liquid scintillation counter (LS6000IC; Beckman Coulter).

Glucose production. Rates of glucose production were measured as described previously (16). Briefly, primary hepatocytes were seeded on 6-well Primaria plates (5×10^5 cells/well) with medium 199 (Invitrogen) containing 10% FBS and 1% penicillin-streptomycin. After cells were allowed to attach for 4 h, the medium was changed to serum-free medium 199. Following 16 h of serum starvation, plates were washed twice with warm Dulbecco's phosphate-buffered saline (DPBS; Sigma-Aldrich). Cells were then incubated for 3 h in glucose- and phenol red-free Dulbecco's modified Eagle's medium (DMEM) (15 mM HEPES, 3.7 g/liter $NaHCO_3$ [pH 7.4]) supplemented with 2 mM sodium pyruvate plus 20 mM sodium lactate or 20 mM glycerol. Glucose concentrations in the medium were measured enzymatically (Sigma-Aldrich). The influence of cyclic AMP (cAMP) was determined by the addition of 0.1 mM 8-(4-chlorophenylthio)adenosine 3′,5′-cyclic monophosphate (pCPT-cAMP; Sigma-Aldrich) during culture and the glucose production assay. PC-TP inhibition was achieved by the addition of 500 nM compound A1 (17) during the glucose production assay.

Glucose oxidation and *de novo* lipogenesis. The conversion of [U-^{14}C]glucose (250 to 360 mCi/mmol; PerkinElmer) to ^{14}C-labeled CO_2 and lipids (i.e., fatty acids and sterols) was measured in order to assess rates of glucose oxidation and *de novo* lipogenesis, respectively (18). Primary hepatocytes were maintained for 4 h in 6-well Primaria plates (5×10^5 cells/well) in medium 199 with 10% FBS and 1% penicillin-streptomycin. Prior to the assay, cells were serum starved for 16 h, washed once with warm DPBS, and incubated for 1 h in glucose-free DMEM. The medium was then changed to high-glucose DMEM containing 2 μCi [U-^{14}C]glucose/ml. After 3 h of incubation, 800 μl of medium was transferred to 15-ml conical tubes. As described above, CO_2 was trapped in NaOH-soaked filter paper that was placed inside the caps of conical tubes. Cells were washed with ice-cold PBS and were scraped with 800 μl of H_2O. Following the addition of 2 ml of 7% KOH in 70% methanol and 3 h of incubation at 90°C, sterols were extracted into 3 ml of petroleum ether. The aqueous phase was then acidified by the addition of 0.8 ml of 10 M H_2SO_4, and fatty acids were extracted using 3 ml of petroleum ether. The petroleum ether was then evaporated under a stream of N_2. Following the addition of Ecoscint H, radioactivity was determined by liquid scintillation counting.

Cellular and mitochondrial O_2 consumption. O_2 consumption rates (OCR) in primary hepatocytes were measured using an XF24 extracellular flux analyzer (Seahorse Bioscience). Primary hepatocytes were seeded on type I collagen-coated XF24 cell culture microplates at a density of 0.25×10^5/well. Following 4 to 5 h of incubation in medium 199 with 10% FBS and 1% penicillin-streptomycin in order to test mitochondrial respiratory function, the culture medium was changed to glucose-free DMEM (pH 7.4 at 37°C) with 1 mM pyruvate. Oligomycin (2 μM), carbonyl cyanide-*p*-trifluoromethoxyphenylhydrazone (FCCP) (1 μM), and 1 μM antimycin A plus 1 μM rotenone were sequentially added to each well during the monitoring of OCR. Oligomycin inhibits ATP synthesis and suppresses respiratory chain function. FCCP is an ionophore that disrupts membrane potential, leading to rapid oxygen consumption. Antimycin A and rotenone are respiratory chain complex inhibitors. For the evaluation of fatty acid oxidation rates, Krebs-Henseleit buffer containing 0.45 g/liter glucose and 0.5 mM carnitine (pH 7.4 at 37°C) was used as the assay medium. OCR values were measured before and after the exposure of cells to 300 μM palmitic acid conjugated with fatty acid-free BSA. To examine the effect of PC-TP inhibition on fatty acid oxidation, cells were sequentially treated with 500 nM compound A1 and 300 μM palmitic acid. For measurements of OCR in mitochondria, mitochondrial pellets were freshly prepared from mouse livers according to the manufacturer's protocol (Seahorse Bioscience). Briefly, livers were minced and homogenized in 10 volumes of mitochondrial isolation buffer containing 70 mM sucrose, 210 mM mannitol, 5 mM HEPES, 1 mM EGTA, and 0.5% fatty acid-free BSA. Homogenates were centrifuged at 800 × *g* for 10 min at 4°C, and the supernatant was filtered with the 70-μm cell strainer. Following the centrifugation of the supernatant at 8,000 × *g* for 10 min at 4°C, the pellets were rinsed again to obtain the mitochondrial fraction. The pellets were resuspended in 70 mM sucrose, 220 mM mannitol, 10 mM KH_2PO_4, 5 mM $MgCl_2$, 2 mM HEPES, 1 mM EGTA, 0.2% BSA, 80 μM palmitoyl-carnitine (Sigma-Aldrich), and 0.5 mM malic acid (Sigma-Aldrich). Mitochondria were seeded in the wells of XF24 cell culture microplates (40 μg protein/well), and OCR values were determined following the sequential injection of 4 mM ADP, 2.5 μg/ml oligomycin, 4 μM FCCP, and 4 μM antimycin.

TCA cycle intermediates. The relative concentrations of TCA cycle intermediates in mitochondria were measured using gas chromatography-mass spectrometry (GC-MS). Briefly, mitochondria were harvested from 0.4 g liver as described above and were resuspended in 100 μl of mitochondrial isolation buffer. The mitochondrial suspension (50 μl) was mixed with 1 ml of a solvent mixture (MeOH-H_2O-$CHCl_3$ [2.5:1:1]) containing 10 μl of 0.5-mg/ml 2-isopropylmalic acid (Sigma-Aldrich) as an internal standard and was shaken at 1,200 rpm for 30 min at 37°C. Following centrifugation at 16,000 × *g* for 3 min at 4°C, 900 μl of the supernatant was mixed with 450 μl of $CHCl_3$. This mixture was centrifuged at 16,000 × *g* for 3 min at 4°C, and 500 μl of the supernatant was mixed with 200 μl of distilled water. Following centrifugation at 16,000 × *g* for 3 min at 4°C, 500 μl of the supernatant was lyophilized and mixed with 20 mg/ml methoxyamine hydrochloride (Sigma-Aldrich) dissolved in pyridine. After shaking at 1,200 rpm for 90 min at 30°C, intermediates were derivatized by the addition of *N*-methyl-*N*-trimethylsilyl trifluoroacetamide (GL Sciences), followed by shaking at 1,200 rpm for 30 min at 37°C. After centrifugation at 16,000 × *g* for 5 min at 4°C, the supernatant was subjected to GC-MS using a GCMS-QP2010 Ultra system (Shimadzu) fitted with a fused silica capillary column (CP-Sil 8 CB Low Bleed/MS; length, 30 m; inner diameter, 0.25 mm; film thickness, 0.25 μm; Agilent). The front inlet temperature was 230°C, and the flow rate of He gas through the column was 39.0 cm/s. The column temperature was maintained at 80°C for 2 min, then increased at a rate of 15°C/min up to 330°C, and then held constant for 6 min. The transfer line and ion source temperatures were 250°C and 200°C, respectively. Data were acquired at a rate of 20 scans per second over an *m/z* range of 85 to 500 using the Advanced Scanning Speed Protocol (Shimadzu).

Cellular ADP/ATP ratio. Hepatocytes were lysed and were incubated for 10 min at 20°C with CellTiter-Glo luminescent cell viability assay reagent (Promega). ATP contents were measured according to relative luminescence units (RLU) using a POLARstar Omega microplate reader (BMG Labtech). For the determination of ADP levels, cell lysates were treated with an ADP-to-ATP converting enzyme (ApoSENSOR ADP/ATP ratio assay kit; BioVision) for 10 min at 20°C directly following the measurement of ATP levels. Final ATP contents, which reflected the sum of cellular ADP and ATP levels, were detected using the CellTiter-Glo luminescent cell viability assay reagent. ADP contents were determined as the difference between the RLU obtained before and after the addition of the ADP-to-ATP converting enzyme.

mRNA expression. Total RNA was extracted from hepatocytes immediately after harvesting using TRIzol reagent (Invitrogen), and cDNA was synthesized with SuperScript III reverse transcriptase (Invitrogen) according to the manufacturer's protocol. Quantitative real-time PCR was performed using a Roche 480 LightCycler (Roche Applied Sciences) with SYBR green (Roche Applied Sciences) detection. The primer sequences used have been reported previously (6).

Protein expression. Total cellular protein was isolated with radioimmunoprecipitation assay (RIPA) buffer (50 mM Tris-HCl, 150 mM NaCl, 1% NP-40, 0.5% sodium deoxycholate, 0.1% sodium dodecyl sulfate [SDS]) supplemented with cOmplete Mini protease inhibitor (Roche Applied Science) and a phosphatase inhibitor tablet (Roche Applied Science). Protein concentrations were determined spectrophotometrically using a Bio-Rad protein assay dye reagent. Equal amounts of proteins were separated by SDS-polyacrylamide gel electrophoresis (PAGE) and were electrophoretically transferred to nitrocellulose membranes (GE Healthcare). The blots were then probed with specific primary antibodies against total AMP-activated protein kinase alpha (AMPKα), phospho-AMPKα (Thr172), total acetyl-CoA carboxylase (ACC), phospho-ACC (Ser79) (Cell Signaling Technology), PC-TP, Them2, and β-actin (4) overnight at 4°C, followed by 1 h of incubation with a horseradish peroxidase (HRP)-conjugated secondary antibody (4). Proteins were visualized by chemiluminescence using the Western Lightning (PerkinElmer) or Super Signal West Dura (Thermo Scientific) substrate.

Immunoprecipitation (IP). Livers were harvested from mice with free access to water that were fed chow or fasted overnight. Liver protein lysates (0.5 mg per 1 ml of RIPA buffer) were precleared by incubation with 10 μl of normal rabbit IgG (Santa Cruz Biotechnology) for 4 h, followed by incubation with 20 μl of Protein G Plus/protein A-agarose beads (50:50 slurry; Calbiochem) for 1 h at 4°C. Beads were pelleted by centrifugation (1,825 × *g* for 10 min at 4°C) and were then discarded. Precleared lysates were then incubated with 10 μl of an anti-PC-TP antibody or 10 μl of normal rabbit IgG as a control for 2 h at 37°C, followed by incubation with 20 μl of Protein G Plus/protein A-agarose beads (50:50 slurry) for 1 h at 37°C. Beads were pelleted by centrifugation (6,000 × *g* for 30 s at 20°C) and were washed 5 times with RIPA buffer by gentle agitation (5 min at 37°C). After the final wash, protein was eluted from the beads, denatured by heating for 5 min at 96°C in 3× Laemmli buffer, and subjected to immunoblot analysis.

Statistical analyses. Data were expressed as means ± standard errors (SE), and differences were evaluated using unpaired Student *t* tests. Differences were considered significant when the *P* value was <0.05.

RESULTS

Them2 promotes fatty acid oxidation, gluconeogenesis, and lipogenesis. We reported previously that plasma β-hydroxybutyrate concentrations were reduced in *Them2*$^{-/-}$ mice (6), a finding suggestive of a role for Them2 in promoting the hepatic oxidation of fatty acids. In the current study, we examined the effects of Them2 expression on hepatocellular fatty acid oxidation (Fig. 1A and B). The lack of Them2 expression reduced the rates of incorporation of [1-^{14}C]palmitate into ASM and CO_2 by 42% and 50%, respectively (Fig. 1A). In keeping with this observation, OCR values were lower in *Them2*$^{-/-}$ hepatocytes than in *Them2*$^{+/+}$ hepatocytes following exposure to palmitic acid (Fig. 1B). To assess whether the loss of Them2 expression was associated with intrinsic alterations in the function of the electron transport chain, OCR in the presence of pyruvate were measured following sequential treatment of hepatocytes with oligomycin, FCCP, and antimycin A plus rotenone (Fig. 1C). In the absence of Them2 expression, basal OCR values were reduced (Fig. 1C, left), as were the areas under the curve (AUC) (Fig. 1C, right). However, Them2 had no effect on other bioenergetic parameters, including maximal OCR values (Fig. 1C). Moreover, Them2 expression had no effect on the function of isolated liver mitochondria (Fig. 1D).

Fatty acid oxidation contributes to efficient gluconeogenesis because it elevates TCA cycle activity and flux through phosphoenolpyruvate carboxykinase (PEPCK), the initial committed step of gluconeogenesis (19, 20). To examine whether reduced fatty acid oxidation in *Them2*$^{-/-}$ hepatocytes was associated with decreased gluconeogenesis, glucose production rates were measured in the presence of the substrates pyruvate and lactate (Fig. 1E). The absence of Them2 was associated with a nonsignificant 23% decrease in basal rates of glucose production but a 41% decrease following stimulation with cAMP. Because it can bypass the TCA cycle, we also tested glycerol as a gluconeogenic substrate (20, 21) in order to determine whether the effect of Them2 was restricted to mitochondria. Them2 expression had no effect on glucose production in the presence of glycerol (Fig. 1E), indicating that decreased TCA cycle activity was most likely responsible for reduced gluconeogenesis in *Them2*$^{-/-}$ hepatocytes.

To determine whether reduced TCA cycle activity would result in reduced rates of glucose oxidation and *de novo* lipogenesis in *Them2*$^{-/-}$ hepatocytes, we measured rates of [U-^{14}C]glucose incorporation into CO_2, as well as into fatty acids and sterols

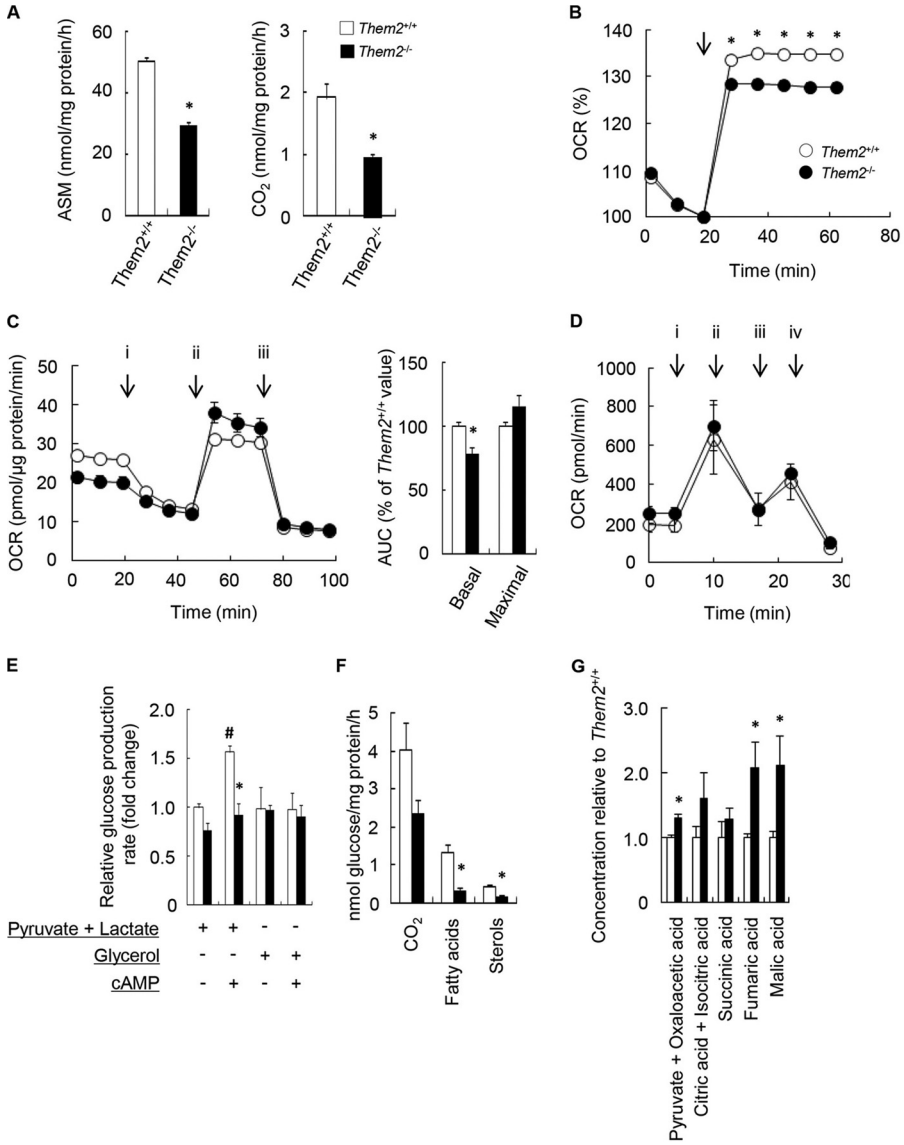

FIG 1 Them2 regulates rates of fatty acid oxidation, gluconeogenesis, and lipogenesis in isolated hepatocytes. (A and B) Fatty acid oxidation rates were determined by measuring the incorporation of [1-^{14}C]palmitate (200 μM) into ASM and CO_2 (A) and the OCR following the addition of 300 μM palmitate (arrow) (B). (C) (Left) Mitochondrial respiratory function was assessed by the influence on OCR of sequential exposure of hepatocytes to oligomycin (2 μM) (i), FCCP (1 μM) (ii), and antimycin A (1 μM) plus rotenone (1 μM) (iii). (Right) AUC for basal (start to i) and maximal (ii to iii) OCR values. For panels A to C, values reflect means of results from 3 determinations, except for OCR values, which reflect means of results from 10 determinations. Each experiment is representative of 3 independent experiments. (D) Mitochondrial fatty acid oxidation was evaluated by measuring OCR in the presence of 80 μM palmitoylcarnitine following the addition of ADP (4 mM) (i), oligomycin (2.5 μg/ml) (ii), FCCP (4 μM) (iii), and antimycin A (4 μM) (iv). (E) Rates of gluconeogenesis were determined by measuring glucose concentrations in culture medium following the addition of gluconeogenic substrates (2 mM pyruvate plus 20 mM lactate or 20 mM glycerol) with or without 0.1 mM cAMP. Baseline values in the presence of pyruvate and lactate (expressed as nmol/mg protein/h) were 350 ± 14 for *Them2*$^{+/+}$ and 268 ± 26 for *Them2*$^{-/-}$ hepatocytes. Baseline values in the presence of glycerol (expressed as nmol/mg protein/h) were 343 ± 77 for *Them2*$^{+/+}$ and 339 ± 17 for *Them2*$^{-/-}$ hepatocytes. (F) Rates of glucose oxidation and *de novo* lipogenesis were determined by measuring the rates of incorporation of [U-^{14}C]glucose (25 mM) into CO_2, fatty acids, and sterols. For panels D to F, values reflect means of results from at least 3 experiments, each of which was performed at least in triplicate. (G) Concentrations of TCA cycle intermediates in mitochondria isolated from mouse livers were quantified by GC-MS. Values represent means of 5 determinations. Where not visualized, error bars are contained within the symbol sizes. An asterisk indicates a significant difference (P, <0.05) between *Them2*$^{+/+}$ and *Them2*$^{-/-}$ hepatocytes; a number sign indicates a significant difference (P, <0.05) between non-cAMP-treated and cAMP-treated cells.

(Fig. 1F). There was a nonsignificant (P, 0.09) 42% decrease in rates of glucose oxidation, as evidenced by reduced incorporation of [U-^{14}C]glucose into CO_2 in hepatocytes cultured from *Them2*$^{-/-}$ mice. In findings indicative of decreased lipogenesis, rates of glucose conversion into fatty acids and sterols were decreased by 78% and 60%, respectively. Taken together, these findings demonstrate that an important hepatocellular function of Them2 is to promote the mitochondrial flux of gluconeogenic and lipogenic substrates through the TCA cycle. Additional evidence for impaired TCA cycle activity was derived from measurements

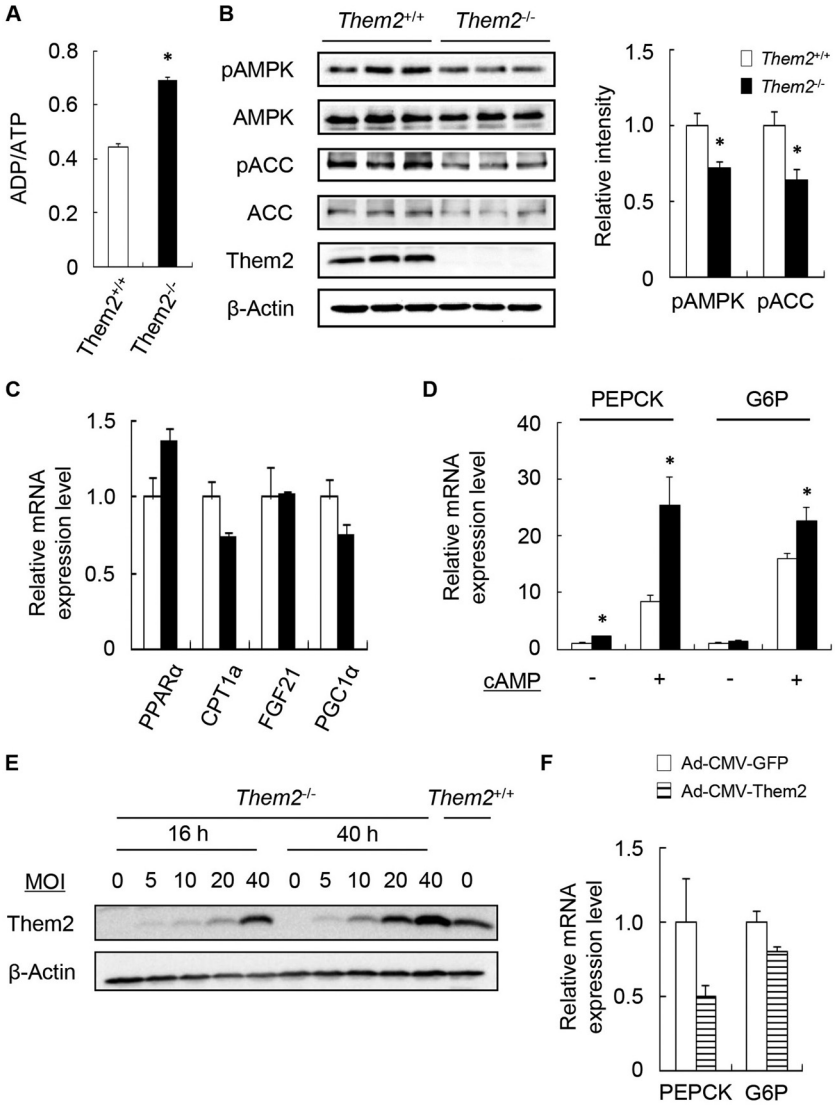

FIG 2 Influence of Them2 expression on ADP/ATP ratios, AMPK activation, and gene expression in isolated hepatocytes. (A to C) Hepatocytes were treated for 6 h with 200 μM BSA-conjugated palmitic acid prior to measurement of ADP/ATP ratios (A), phosphoprotein and total-protein levels (with quantification by densitometry after normalization of phosphoprotein expression to expression of the corresponding total protein) (B), and mRNA levels (C). (D) Hepatocytes were incubated for 3 h in a gluconeogenic medium containing 2 mM pyruvate plus 20 mM lactate with or without 0.1 mM cAMP and were then harvested to determine mRNA levels. (E) Them2 expression was determined by immunoblot analysis following exposure to recombinant Ad-CMV-Them2 for 16 or 40 h at the indicated MOI. (F) Hepatocytes were infected with recombinant Ad-CMV-Them2 or Ad-CMV-GFP at an MOI of 40. Sixteen hours postinfection, hepatocytes were incubated for 3 h in a gluconeogenic medium with 0.1 mM cAMP; then they were harvested for the determination of mRNA levels. For panels A and F, values represent means of results from 4 determinations. For panels B and C, means represent results of ≥3 determinations. Both experiments are representative of 2 or 3 independent experiments. For panel D, values are means of results for 6 to 9 samples generated in 2 or 3 independent experiments. An asterisk indicates a significant difference (P, <0.05) between *Them2*$^{+/+}$ and *Them2*$^{-/-}$ hepatocytes.

of TCA cycle intermediates in mitochondria isolated from livers. The absence of Them2 was associated with increased steady-state concentrations of pyruvate plus oxaloacetate, fumarate, and malate (Fig. 1G).

In findings consistent with reduced rates of fatty acid oxidation, ADP/ATP ratios were increased in *Them2*$^{-/-}$ hepatocytes (Fig. 2A). AMPK promotes fatty acid oxidation by phosphorylating ACC. This reduces the production of malonyl-CoA, which inhibits carnitine palmitoyltransferase 1a (CPT1a) (22). Notwithstanding the increase in ADP/ATP ratios, deletion of Them2 decreased phospho-AMPK (pAMPK)/total-AMPK ratios and pACC/total-ACC ratios by 28% and 36%, respectively (Fig. 2B). These data suggest that reduced AMPK signaling might have contributed, at least in part, to decreased fatty acid oxidation in *Them2*$^{-/-}$ hepatocytes.

Experiments with *Them2*$^{-/-}$ mice suggested that Them2 might promote the hepatic oxidation of fatty acids by activation of PPARα (6). Apart from a modest nonsignificant (P, 0.08) decrease in CPT1a levels under the current experimental conditions, we observed no appreciable changes in mRNA expression levels of PPARα or its target genes, encoding fibroblast growth factor 21 (FGF21) and peroxisome proliferator-activated receptor γ coacti-

vator 1α (PGC1α) (23–26), in *Them2*$^{-/-}$ hepatocytes (Fig. 2C). Notwithstanding reduced rates of gluconeogenesis, mRNA levels of PEPCK and glucose-6-phosphatase (G6P) were increased in the absence of Them2 expression (Fig. 2D), in keeping with the likelihood that attenuated gluconeogenesis in *Them2*$^{-/-}$ hepatocytes is a consequence of reduced TCA cycle activity. To determine whether the upregulation of these genes could be attributable to compensatory changes, we used an adenovirus to rescue the expression of Them2. Figure 2E shows that Them2 expression was restored in *Them2*$^{-/-}$ hepatocytes at 16 h following Ad-CMV-Them2 infection at a multiplicity of infection (MOI) of 40. Acute restoration of Them2 expression resulted in a trend toward decreased mRNA expression of PEPCK and G6P (Fig. 2F).

PC-TP promotes fatty acid oxidation and gluconeogenesis. The enzymatic activity of Them2 is enhanced by interactions with PC-TP (3), and *Pctp*$^{-/-}$ mice exhibit key similarities to *Them2*$^{-/-}$ mice, including reduced plasma β-hydroxybutyrate concentrations (11). To marshal evidence for a regulatory role for PC-TP in Them2-mediated effects on TCA cycle activity, we subjected *Pctp*$^{-/-}$ hepatocytes to a similar series of measurements. As observed in *Them2*$^{-/-}$ hepatocytes, lack of PC-TP expression reduced the incorporation of [1-^{14}C]palmitate into ASM and CO_2 by 29% and 43%, respectively (Fig. 3A). OCR values were also lower in *Pctp*$^{-/-}$ hepatocytes following exposure to palmitic acid (Fig. 3B). In the presence of pyruvate, the loss of PC-TP expression was associated with nonsignificant reductions in basal OCR (Fig. 3C). However, maximal values were increased in *Pctp*$^{-/-}$ hepatocytes, a result indicative of enhanced mitochondrial respiratory capacity in the absence of PC-TP expression (Fig. 3C). As observed in the absence of Them2, PC-TP expression had no effect on the function of isolated liver mitochondria (Fig. 3D).

As with *Them2*$^{-/-}$ hepatocytes, basal glucose production rates tended to be reduced (*P*, 0.07) by 33% in *Pctp*$^{-/-}$ hepatocytes (Fig. 3E), whereas there was a marked (40%) reduction in cAMP-stimulated glucose production rates. In keeping with the effects of Them2 expression, PC-TP expression had no effect on glucose production in the presence of glycerol (Fig. 3E), indicating that decreased TCA cycle activity was most likely responsible for the reduction in gluconeogenesis in *Pctp*$^{-/-}$ hepatocytes. In contrast to observations with *Them2*$^{-/-}$ hepatocytes, PC-TP had no effect on rates of [U-^{14}C]glucose incorporation into CO_2, fatty acids, or sterols (Fig. 3F). Moreover, steady-state concentrations of TCA cycle intermediates were unchanged in mitochondria isolated from *Pctp*$^{-/-}$ mice (Fig. 3G). These data suggest that mitochondrial metabolism is only partially affected by PC-TP expression.

In keeping with reduced rates of fatty acid oxidation, ADP/ATP ratios were increased in *Pctp*$^{-/-}$ hepatocytes (Fig. 4A), as was observed for *Them2*$^{-/-}$ hepatocytes. The pAMPK/total-AMPK ratios were also slightly decreased, but there were no changes in the pACC/total-ACC ratios (Fig. 4B). In contrast to the findings for *Them2*$^{-/-}$ hepatocytes, loss of PC-TP expression was associated with marked increases in mRNA levels of CPT1a, FGF21, and PGC1α (Fig. 4C), notwithstanding decreased rates of fatty acid oxidation. Expression of Them2 mRNA (Fig. 4C) and protein (Fig. 4B) was reduced in the absence of PC-TP expression. In contrast to those in *Them2*$^{-/-}$ hepatocytes, mRNA levels of the gluconeogenic PEPCK and G6P genes were unchanged in the absence of PC-TP expression (Fig. 4D). Taken together, these findings strongly suggest that PC-TP regulates Them2 activity in hepatocytes but that transcriptionally mediated adaptive changes in fatty acid metabolism may partially compensate for the regulatory effects. To assess whether these were compensatory changes, we used an adenovirus to rescue the expression of PC-TP. Figure 4E shows that PC-TP expression was restored in *Pctp*$^{-/-}$ hepatocytes at 16 h following Ad-CMV-PC-TP infection at an MOI of 5. However, the restoration of PC-TP in *Pctp*$^{-/-}$ hepatocytes neither rescued Them2 expression nor reduced the expression of PPARα target genes (Fig. 4F).

Requirement for Them2 in PC-TP-mediated regulation of mitochondrial metabolism. To provide further evidence for a regulatory effect of PC-TP on Them2 and to exclude the possibility that reduced rates of fatty acid oxidation in *Pctp*$^{-/-}$ hepatocytes reflected chronic adaptation, we utilized compound A1, a small-molecule inhibitor that rapidly inactivates PC-TP by competitively inhibiting phosphatidylcholine binding, increasing the thermal stability of the protein and disrupting its interactions with Them2 (10, 17, 27). In results consistent with a direct effect of PC-TP on fatty acid oxidation, compound A1 reduced OCR values in the presence of palmitic acid in *Pctp*$^{+/+}$ hepatocytes but not in *Pctp*$^{-/-}$ hepatocytes (Fig. 5A). Also indicative of the requirement of Them2 expression for PC-TP-mediated regulation was the finding that OCR values were reduced in *Them2*$^{+/+}$ but not in *Them2*$^{-/-}$ hepatocytes (Fig. 5B).

In *Pctp*$^{+/+}$ and *Them2*$^{+/+}$ hepatocytes, compound A1 suppressed basal but not cAMP-stimulated glucose production rates when pyruvate and lactate were utilized as gluconeogenic substrates (Fig. 5C and D). These effects were not observed in hepatocytes lacking either PC-TP or Them2. Also consistent with an effect of PC-TP on TCA cycle flux was the finding that the rates of glycerol gluconeogenesis were not affected by chemical inhibition of PC-TP (i.e., a nonsignificant 3.5% ± 4.4% reduction). These findings suggest that fully elevated TCA cycle activity could compensate for the partial defect in fatty acid oxidation.

As observed in *Pctp*$^{-/-}$ hepatocytes, compound A1 reduced AMPK phosphorylation without affecting the phosphorylation of ACC (Fig. 6A). However, under conditions of short-term chemical inactivation of PC-TP, we no longer observed increases in the expression of genes that promote fatty acid oxidation (Fig. 6B). Nor were there changes in the expression of Them2 mRNA or protein (Fig. 6A and B). As in the absence of PC-TP expression, there was no effect of PC-TP inhibition on gluconeogenic gene expression (Fig. 6C and D).

The observations that Them2 expression and PC-TP expression similarly promote fatty acid oxidation and gluconeogenesis, but that only Them2 expression promotes lipogenesis, suggest the possibility that a Them2–PC-TP complex plays a primarily regulatory role in cellular metabolism under fasting conditions but that Them2 might act independently under fed conditions. To further test these possibilities, we examined the expression levels of Them2 and PC-TP, as well as their interactions, under fed and fasting conditions (Fig. 7). Whereas Them2 expression and PC-TP expression were not appreciably affected by fasting or feeding, there were marked increases in Them2–PC-TP interactions during fasting, as evidenced by a 3.2-fold increase in the coimmunoprecipitation of Them2 by PC-TP.

DISCUSSION

This study was designed to understand the metabolic role of Them2 in the liver and its regulation by PC-TP. The main findings were as follows: (i) rates of fatty acid oxidation and gluconeogen-

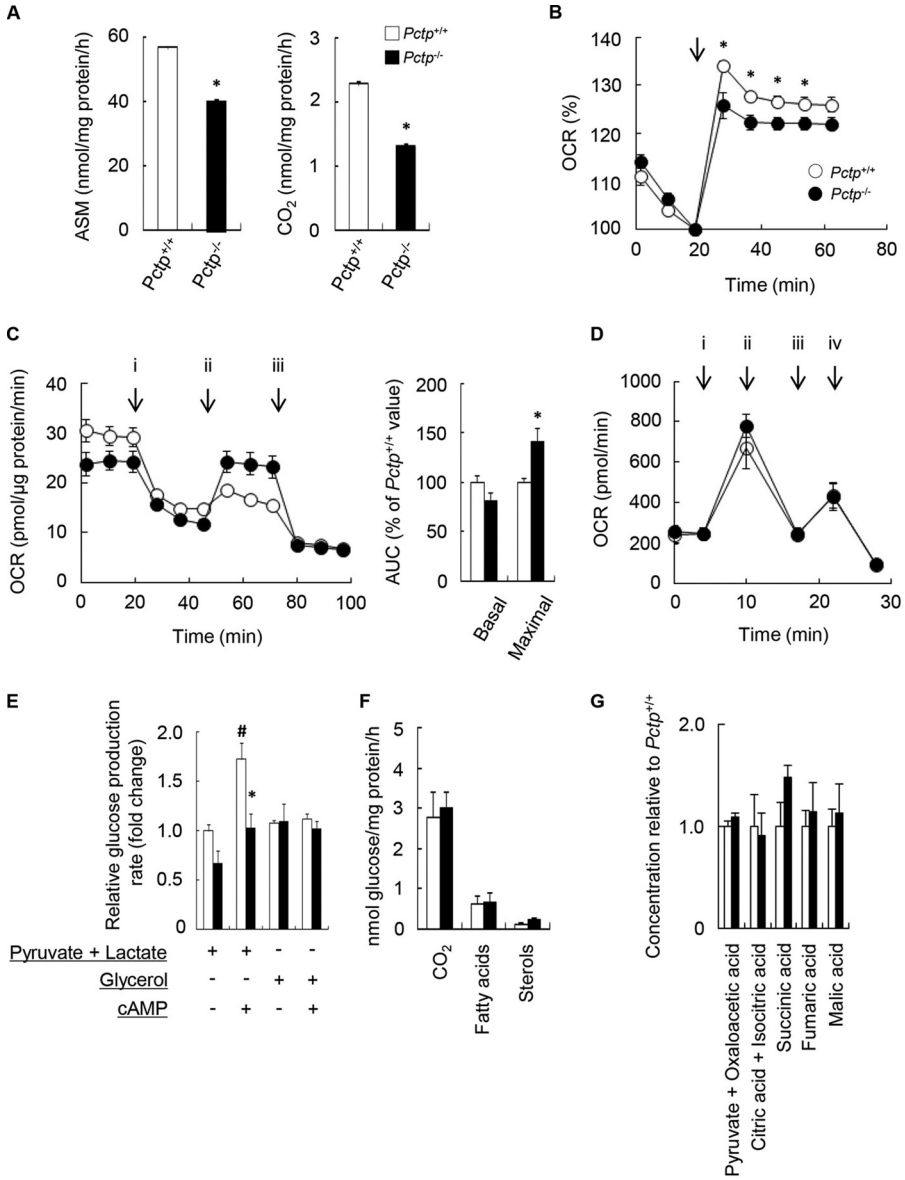

FIG 3 PC-TP regulates rates of fatty acid oxidation and gluconeogenesis but not lipogenesis in isolated hepatocytes. (A and B) Fatty acid oxidation rates were determined by measuring the incorporation of [1-^{14}C]palmitate (200 μM) into ASM and CO_2 (A) and the OCR following the addition of 300 μM palmitate (arrow) (B). (C) (Left) Mitochondrial respiratory function was assessed by measuring OCR following sequential exposure of hepatocytes to oligomycin (2 μM) (i), FCCP (1 μM) (ii), and antimycin A (1 μM) plus rotenone (1 μM) (iii). (Right) AUC for basal (start to i) and maximal (ii to iii) OCR values. For panels A to C, values represent means of results from 3 determinations, except for OCR values, which reflect means of results from 10 determinations. Each experiment is representative of 3 independent experiments. (D) Mitochondrial fatty acid oxidation was evaluated by measuring OCR in the presence of 80 μM palmitoylcarnitine following the addition of ADP (4 mM) (i), oligomycin (2.5 μg/ml) (ii), FCCP (4 μM) (iii), and antimycin A (4 μM) (iv). (E) Rates of gluconeogenesis were determined by measuring glucose concentrations in culture medium following the addition of gluconeogenic substrates (2 mM pyruvate plus 20 mM lactate or 20 mM glycerol) with or without 0.1 mM cAMP. Baseline values in the presence of pyruvate and lactate (expressed as nmol/mg protein/h) were 559 ± 34 for *Pctp*$^{+/+}$ and 376 ± 68 for *Pctp*$^{-/-}$ hepatocytes. Baseline values in the presence of glycerol (expressed as nmol/mg protein/h) were 602 ± 18 for *Pctp*$^{+/+}$ and 616 ± 95 for *Pctp*$^{-/-}$ hepatocytes. (F) Rates of glucose oxidation and *de novo* lipogenesis were determined by measuring the incorporation of [U-^{14}C]glucose (25 mM) into CO_2, fatty acids, and sterols. For panels D to F, values reflect means of results from at least 3 experiments, each of which was performed at least in triplicate. (G) Concentrations of TCA cycle intermediates in isolated mitochondria were quantified by GC-MS. Values represent means of results from 5 determinations. Where not visualized, error bars are contained within the symbol sizes. An asterisk indicates a significant difference (P, <0.05) between *Pctp*$^{+/+}$ and *Pctp*$^{-/-}$ hepatocytes; a number sign indicates a significant difference (P, <0.05) between non-cAMP-treated and cAMP-treated cells.

esis were decreased by genetic ablation of Them2 or PC-TP, despite preserved mitochondrial function; (ii) the absence of Them2 but not PC-TP expression was associated with decreased rates of glucose oxidation and lipogenesis; (iii) the absence of PC-TP but not Them2 expression was associated with increases in the expression of PPARα and its target genes that promote fatty acid oxidation; and (iv) chemical inhibition of PC-TP reduced fatty acid oxidation and gluconeogenesis only in the presence of Them2. Taken together, these findings provide evidence for key roles of Them2 and PC-TP in promoting hepatic TCA cycle activity.

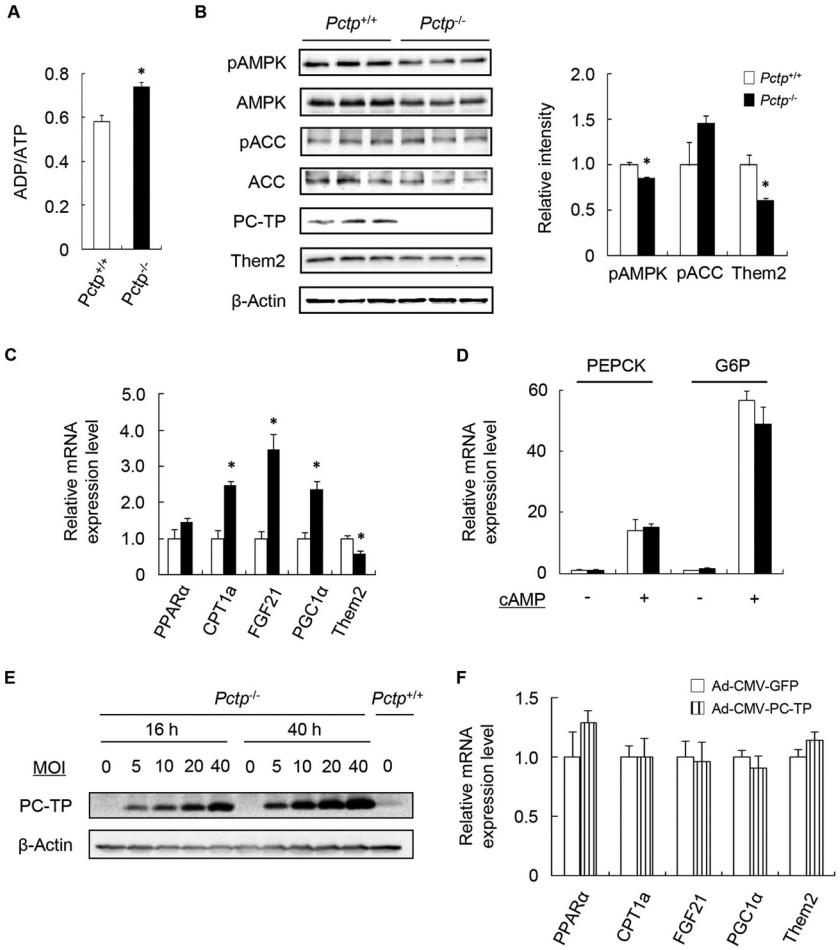

FIG 4 Influence of PC-TP expression on ADP/ATP ratios, AMPK activation, and gene expression in isolated hepatocytes. (A to C) Hepatocytes were treated for 6 h with 200 μM BSA-conjugated palmitic acid prior to measurement of ADP/ATP ratios (A), phosphoprotein and total-protein levels (with quantification by densitometry after normalization of phosphoprotein expression to expression of the corresponding total protein and of Them2 to β-actin) (B), and mRNA levels (C). (D) Hepatocytes were incubated for 3 h in a gluconeogenic medium containing 2 mM pyruvate plus 20 mM lactate with or without 0.1 mM cAMP and were then harvested to determine mRNA levels. (E) PC-TP expression was determined by immunoblot analysis following exposure to recombinant Ad-CMV-PC-TP for 16 or 40 h at the indicated MOI. (F) Hepatocytes were infected with recombinant Ad-CMV-PC-TP or Ad-CMV-GFP at an MOI of 5. Sixteen hours later, hepatocytes were treated for 6 h with 200 μM BSA-conjugated palmitic acid; they were then harvested for the determination of mRNA levels. For panels A and F, values represent means of results from 4 determinations. For panels B and C, values represent means of results from ≥3 determinations. Both experiments are representative of 2 or 3 independent experiments. For panel D, values are means of results for 6 to 9 samples generated in 2 or 3 independent experiments. An asterisk indicates a significant difference (P, <0.05) between $Pctp^{+/+}$ and $Pctp^{-/-}$ hepatocytes.

The mitochondrial uptake of fatty acids requires their conversion to acyl-CoA molecules (26). CPT1a is the transporter on the outer mitochondrial membrane that catalyzes the initial step in the uptake of fatty acyl-CoA esters. Considering that CPT1a resides with long-chain acyl-CoA synthetase (ACSL) on mitochondria (28), the uptake of fatty acids appears to be coupled mechanistically to esterification to CoA (29). A requirement for newly esterified fatty acyl-CoA esters would imply that cytosolic fatty acyl-CoA esters must be converted to free fatty acids and then newly reesterified. The reduced rates of fatty acid oxidation in $Them2^{-/-}$ and $Pctp^{-/-}$ hepatocytes suggest a role for a Them2–PC-TP complex in providing ACSL with both free fatty acids and CoA substrates to facilitate their esterification and mitochondrial uptake.

Our data suggest that Them2-mediated oxidation of fatty acids is required for efficient gluconeogenesis. This is consistent with observations in mice (13) and in humans (30) of hypoglycemia due to reduced gluconeogenesis in the setting of impaired fatty acid oxidation, as well as with our prior reports that both $Them2^{-/-}$ and $Pctp^{-/-}$ mice exhibit lower rates of hepatic glucose production when fed a high-fat diet (6, 17). The effects of genetic ablation of Them2 and PC-TP on cAMP-stimulated rates of gluconeogenesis were more striking than the modest effects on basal rates, likely because cAMP enhances not only gluconeogenesis but also fatty acid oxidation (31). This possibility is supported by the lack of a significant effect of compound A1 on rates of gluconeogenesis following treatment of hepatocytes with cAMP, which would not likely alter TCA flux in the short term.

When glucose was provided to cells as the energy source, the expression of Them2, but not that of PC-TP, promoted glucose oxidation along with glucose-derived lipogenesis. Once taken up into hepatocytes, glucose is processed by glycolysis to pyruvate, which enters the TCA cycle for oxidation. Excess TCA cycle inter-

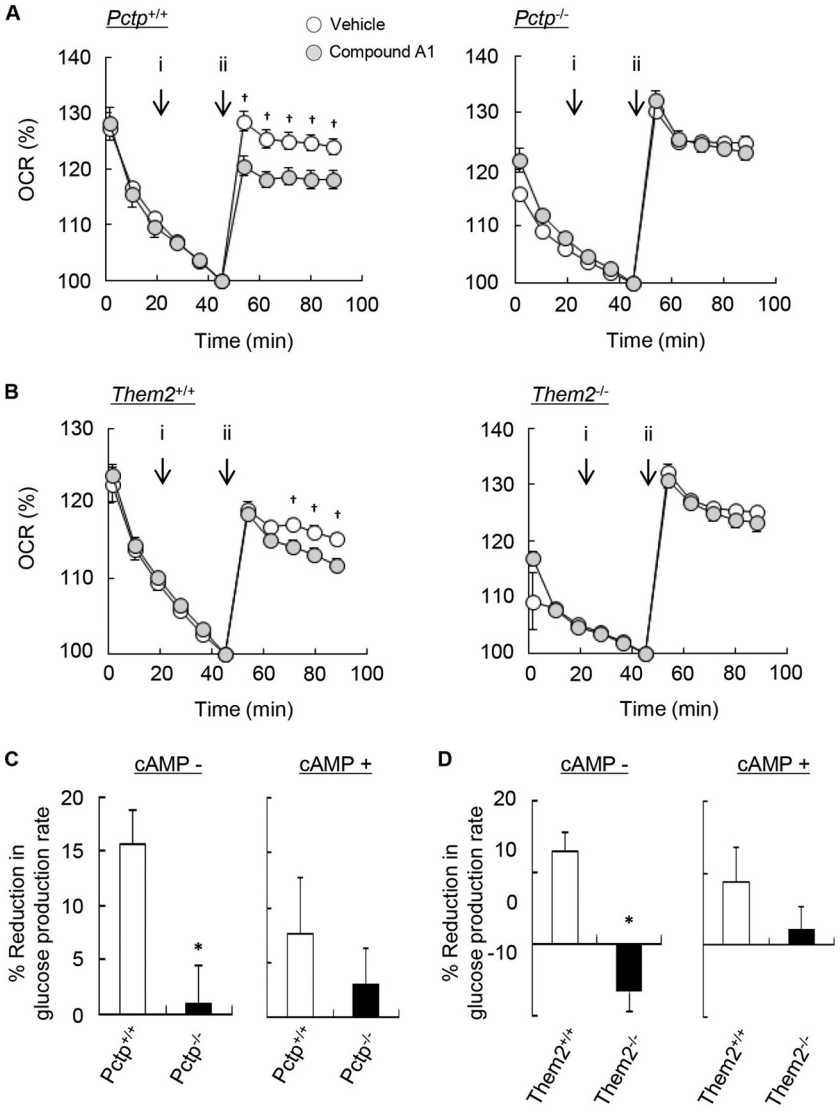

FIG 5 Chemical inactivation of PC-TP leads to Them2-dependent suppression of fatty acid oxidation and gluconeogenesis in isolated hepatocytes. (A and B) Hepatocytes were treated with a vehicle (dimethyl sulfoxide at a final concentration of 0.0025%) or 500 nM compound A1 (i), and then the influence of PC-TP (A) or Them2 (B) expression on OCR was determined following the addition of 300 μM palmitic acid (ii) as indicated by the arrow. Values reflect means of results from 10 determinations of OCR, and each experiment is representative of 3 independent experiments. (C and D) The influence of PC-TP (C) and Them2 (D) expression on the compound A1-induced reduction in gluconeogenesis was assessed by measuring rates of basal and cAMP-stimulated glucose production in the presence of 2 mM pyruvate plus 20 mM lactate and 500 nM compound A1. Baseline values in the absence of cAMP (expressed as nmol/mg protein/h) were as follows: 304 ± 21 for $Pctp^{+/+}$ and 476 ± 93 for $Pctp^{-/-}$ hepatocytes; 262 ± 26 for $Them2^{+/+}$ and 296 ± 48 for $Them2^{-/-}$ hepatocytes. Baseline values in the presence of cAMP (expressed as nmol/mg protein/h) were as follows: 550 ± 28 for $Pctp^{+/+}$ and 433 ± 43 for $Pctp^{-/-}$ hepatocytes; 429 ± 39 for $Them2^{+/+}$ and 453 ± 69 for $Them2^{-/-}$ hepatocytes. Values reflect means of results from at least 3 experiments, each of which was performed in triplicate. Where not visualized, error bars are contained within the symbol sizes. A dagger indicates a significant difference (P, <0.05) between compound A1 and the vehicle control; an asterisk indicates a significant difference (P, <0.05) between $Pctp^{+/+}$ and $Pctp^{-/-}$ hepatocytes or between $Them2^{+/+}$ and $Them2^{-/-}$ hepatocytes.

mediates are diverted out of mitochondria as citrate, which is utilized for *de novo* lipogenesis (32). Accordingly, lower rates of both glucose oxidation and lipogenesis *de novo* in $Them2^{-/-}$ hepatocytes are most likely explained by impaired TCA cycle activity in the absence of Them2 expression. This was evidenced both by reduced basal OCR values in $Them2^{-/-}$ hepatocytes incubated in the presence of pyruvate and by compensatory changes in the concentrations of TCA cycle intermediates. In keeping with these findings, increased hepatic fatty acyl-CoA concentrations, which were observed previously in the livers of $Them2^{-/-}$ mice (6), would be expected to reduce glucose utilization by inhibiting phosphofructokinase activity (33). These effects were not observed in $Pctp^{-/-}$ hepatocytes, suggesting that Them2–PC-TP interactions are not involved in regulating glucose oxidation and lipogenesis.

A notable difference between $Them2^{-/-}$ and $Pctp^{-/-}$ hepatocytes was the upregulation of PPARα target genes in $Pctp^{-/-}$ hepatocytes. Because fatty acid oxidation rates were decreased in the absence of PC-TP expression, this upregulation most likely reflected a long-term compensatory effect. This possibility is sup-

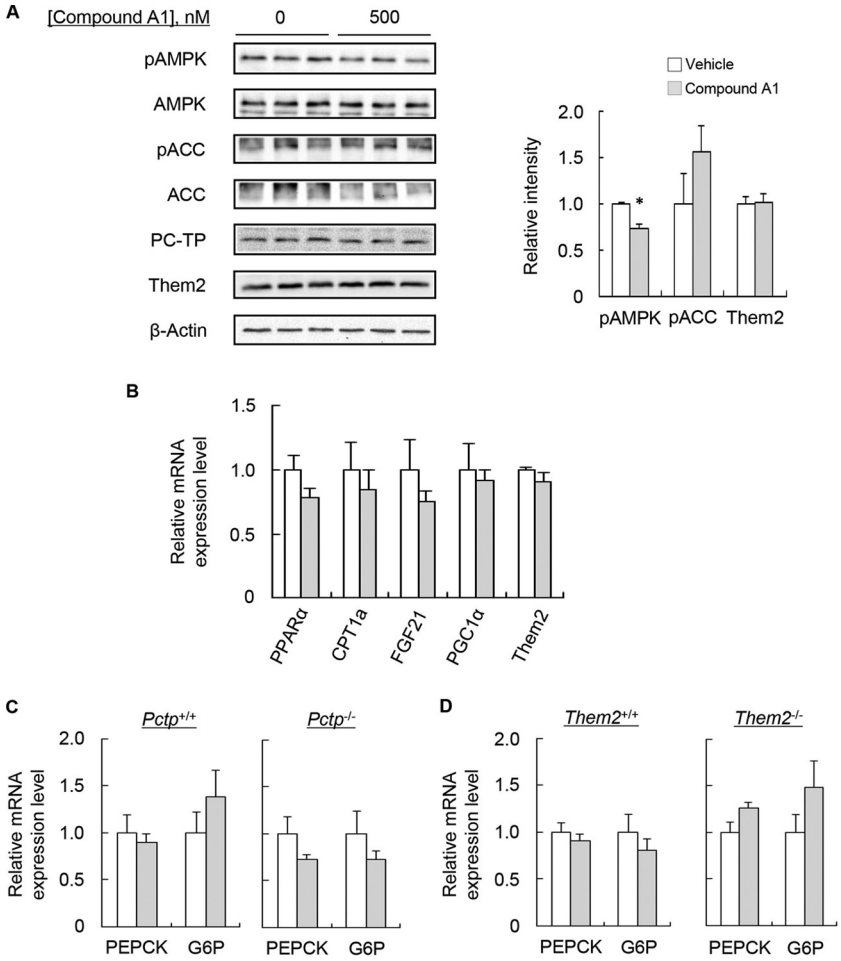

FIG 6 Influence of PC-TP inhibition on gene expression and AMPK activation in isolated hepatocytes. (A and B) Hepatocytes were incubated for 6 h in serum-free Williams' medium E containing 200 μM BSA-conjugated palmitic acid with a vehicle (dimethyl sulfoxide at a final concentration of 0.0025%) or 500 nM compound A1 and were then harvested to determine phosphoprotein and total-protein levels (with quantification by densitometry after normalization of phosphoprotein expression to corresponding total-protein expression and of Them2 to β-actin) (A) and mRNA levels (B). Means represent results of ≥3 determinations. Both experiments are representative of 2 or 3 independent experiments. (C and D) Hepatocytes were incubated for 3 h in glucose-free DMEM containing 2 mM pyruvate plus 20 mM lactate with a vehicle (dimethyl sulfoxide at a final concentration of 0.0025%) or 500 nM compound A1 and were then harvested for the determination of mRNA levels. Values are means of results for 6 samples generated in 2 independent experiments. An asterisk indicates a significant difference (P, <0.05) between compound A1 and the vehicle control.

ported by the finding that acute restoration of PC-TP expression using a recombinant adenovirus did not reverse the increases in PPARα target gene expression in *Pctp*$^{-/-}$ hepatocytes. Because PGC1α promotes mitochondrial biogenesis (34), upregulation of PGC1α presumably explains the increase in maximal OCR values in the absence of PC-TP expression. Under these conditions, lower rates of fatty acid oxidation in *Pctp*$^{-/-}$ hepatocytes were most likely attributable to reduced Them2 expression, as well as to suboptimal Them2 activity in the absence of PC-TP. The lack of upregulation of PPARα target genes in *Them2*$^{-/-}$ hepatocytes may be explained on the basis of reduced AMPK activity, which also promotes the activity of PPARα (35). Although there were modest reductions in AMPK activity in *Pctp*$^{-/-}$ hepatocytes, these were not accompanied by reduced phosphorylation of ACC, a key target of AMPK. This possibility is further supported by increased mRNA levels of PEPCK and G6P in *Them2*$^{-/-}$ but not *Pctp*$^{-/-}$ hepatocytes (36). Because ADP/ATP ratios were increased in the setting of reduced rates of fatty acid oxidation, reduced AMPK activity was likely attributable to inhibition by fatty acyl-CoA esters (37), which accumulate in mouse liver in the absence of Them2 but not in the absence of PC-TP (6, 9).

In support of a regulatory role of a Them2–PC-TP complex in TCA cycle activity, compound A1 suppressed both fatty acid oxidation and basal rates of gluconeogenesis only when both proteins were expressed in hepatocytes. We have demonstrated previously that compound A1 inactivates PC-TP without altering its expression (10, 17) and dissociates the Them2–PC-TP complex (10). In keeping with this mechanism, compound A1-mediated reductions in fatty acid oxidation and gluconeogenesis were most likely mediated by the effects of PC-TP on Them2 activity. In contrast to the genetic deletion of PC-TP, PPARα target genes were not activated in the setting of acute PC-TP inhibition. This further supports the likelihood that increased mRNA levels of PPARα target genes observed in *Pctp*$^{-/-}$ hepatocytes represented compensatory responses to chronic decreases in rates of fatty acid oxidation.

Our data, when taken together with prior observations in

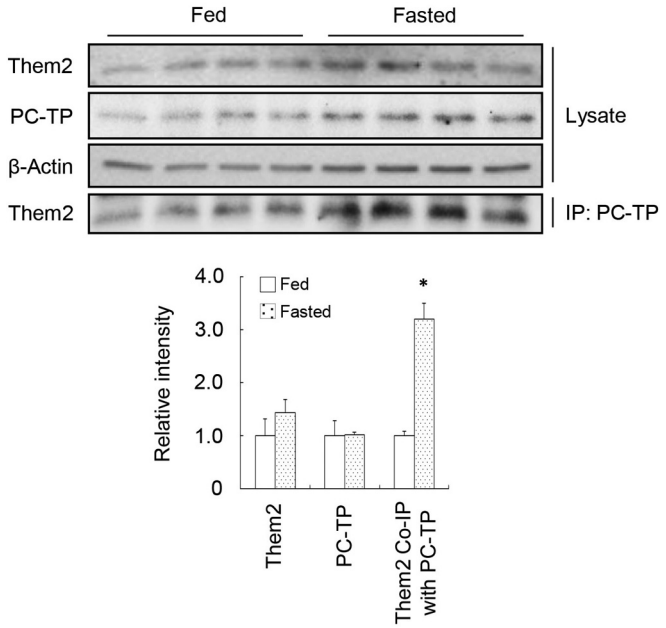

FIG 7 Increased Them2–PC-TP interactions in the liver during fasting. Wild-type FVB/NJ mice either were fed chow or were fasted overnight prior to harvesting of livers. Expression levels of Them2 and PC-TP were determined by immunoblot analysis and were quantified by densitometry after normalization to β-actin. The amounts of Them2 pulled down by immunoprecipitation of PC-TP were quantified by densitometry for fasted and fed mice. Data are representative of results from 2 independent experiments. The asterisk indicates a significant difference (P, <0.05) between fasted and fed mice.

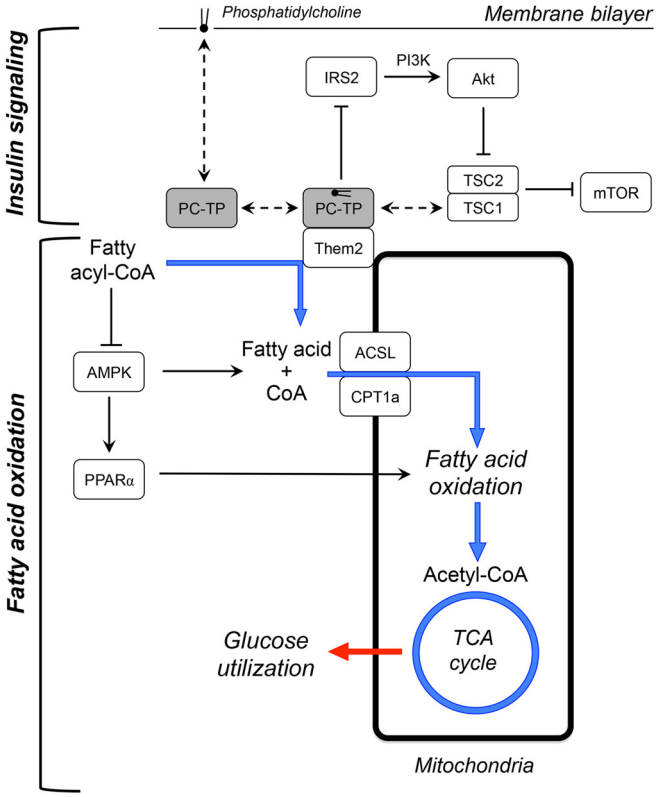

FIG 8 Schematic model for metabolic regulation by Them2 and PC-TP in hepatocytes. A complex of Them2 and PC-TP is postulated to regulate nutrient homeostasis within hepatocytes by suppressing insulin signaling and promoting fatty acid oxidation. Fasting promotes the interactions between Them2 and PC-TP. This could be attributable to PPARα-mediated enrichment of membranes with unsaturated phosphatidylcholines (38–40), which may induce conformational changes in PC-TP that favor binding to Them2 (12). (Top) As described previously (10), the Them2–PC-TP complex limits insulin signaling by decreasing IRS2 activation and stabilizing the TSC1–TSC2 complex, which suppresses mTOR. (Adapted from *Science Signaling* [10].) (Bottom) The Them2–PC-TP complex also catalyzes the hydrolysis of fatty acyl-CoA esters to free fatty acids and CoA, which are then reesterified by ACSL and transported by CPT1a into mitochondria for oxidation. Because fatty acyl-CoA esters inhibit AMPK (37), their hydrolysis leads to activation of the kinase, which increases the activities of both CPT1a and PPARα, further promoting fatty acid oxidation. The overall effect of the Them2–PC-TP complex is to enhance TCA cycle activity. Under fasting conditions, this increases rates of gluconeogenesis. Under fed conditions (not shown), when hepatocellular glucose concentrations are high, Them2–PC-TP interactions are reduced. In this setting, the Them2-mediated increases in TCA cycle activity are still sufficient to promote glucose oxidation and *de novo* lipogenesis. Dashed arrows indicate binding events; solid arrows indicate stimulation; solid lines with line stops indicate inhibition. The blue arrows trace the metabolic fate of fatty acids, and the red arrow represents the influence of TCA cycle activity on glucose utilization. PI3K, phosphoinositide 3-kinase.

Them2$^{-/-}$ and *Pctp*$^{-/-}$ mice, suggest the mechanistic model proposed in Fig. 8. As we have reported recently (10), a complex of Them2–PC-TP suppresses insulin signaling by reducing the activation of IRS2, as well as by stabilizing the tuberous sclerosis 1 (TSC1)–TSC2 complex, which suppresses mTOR activity. In the presence of increased hepatocellular fatty acid concentrations, as is the case during fasting, PC-TP stimulates Them2-mediated hydrolysis of fatty acyl-CoA esters to free fatty acids, which are reesterified by ACSL and channeled by CPT1a for mitochondrial oxidation. This promotes TCA cycle activity, which in turn facilitates gluconeogenesis. In contrast, in the presence of high glucose concentrations during feeding, Them2-mediated increases in TCA cycle activity promote glucose oxidation (not shown in Fig. 8). This, together with increased TCA cycle activity, leads to increased *de novo* lipogenesis.

The marked increases in Them2–PC-TP interactions in the livers of fasted mice are in keeping with the model in Fig. 8, as well as with our prior proposal that this interaction may be enhanced by conformational changes in PC-TP that occur upon the binding of phosphatidylcholines with more unsaturated fatty acyl chains (10, 12). In this connection, PPARα activation promotes the synthesis of polyunsaturated fatty acids (38, 39) and modulates the molecular species of phosphatidylcholines in the liver (40).

In contrast to what is observed in hepatocytes in hepatocytes, Them2 and PC-TP in brown adipocytes reduce rates of norepinephrine-stimulated fatty acid oxidation (4, 7). Whereas reciprocal regulation of fatty acid oxidation in the liver and brown adipose tissue is in keeping with the role of the liver in supplying nutrients to oxidative tissue during fasting, this would also suggest that Them2 and PC-TP regulate the access of fatty acyl-CoA molecules to mitochondria by distinct molecular mechanisms in these two tissues. Studies using mice with tissue-specific deletion of Them2 and PC-TP may be expected to help dissect these mechanisms of metabolic regulation.

ACKNOWLEDGMENTS

The work was supported by National Institutes of Health grants R37 DK48873 and R01 DK56626 to D.E.C. and the Harvard Digestive Diseases

Center (P30 DK034854). Y.K. was funded in part by a grant from the Ministry of Education, Culture, Sports, Science, and Technology of Japan (Global COE Program Global Center of Excellence for Education and Research on Signal Transduction Medicine in the Coming Generation). B.A.E. was funded in part by a Liver Scholar Award from the American Association for the Study of Liver Diseases.

REFERENCES

1. **Wei J, Kang HW, Cohen DE.** 2009. Thioesterase superfamily member 2 (Them2)/acyl-CoA thioesterase 13 (Acot13): a homotetrameric hotdog fold thioesterase with selectivity for long-chain fatty acyl-CoAs. Biochem. J. **421:**311–322. http://dx.doi.org/10.1042/BJ20090039.
2. **Cao J, Xu H, Zhao H, Gong W, Dunaway-Mariano D.** 2009. The mechanisms of human hotdog-fold thioesterase 2 (hTHEM2) substrate recognition and catalysis illuminated by a structure and function based analysis. Biochemistry **48:**1293–1304. http://dx.doi.org/10.1021/bi801879z.
3. **Kanno K, Wu MK, Agate DS, Fanelli BJ, Wagle N, Scapa EF, Ukomadu C, Cohen DE.** 2007. Interacting proteins dictate function of the minimal START domain phosphatidylcholine transfer protein/StarD2. J. Biol. Chem. **282:**30728–30736. http://dx.doi.org/10.1074/jbc.M703745200.
4. **Kang HW, Ribich S, Kim BW, Hagen SJ, Bianco AC, Cohen DE.** 2009. Mice lacking Pctp/StarD2 exhibit increased adaptive thermogenesis and enlarged mitochondria in brown adipose tissue. J. Lipid Res. **50:**2212–2221. http://dx.doi.org/10.1194/jlr.M900013-JLR200.
5. **Cheng Z, Bao S, Shan X, Xu H, Gong W.** 2006. Human thioesterase superfamily member 2 (hTHEM2) is co-localized with beta-tubulin onto the microtubule. Biochem. Biophys. Res. Commun. **350:**850–853. http://dx.doi.org/10.1016/j.bbrc.2006.09.105.
6. **Kang HW, Niepel MW, Han S, Kawano Y, Cohen DE.** 2012. Thioesterase superfamily member 2/acyl-CoA thioesterase 13 (Them2/Acot13) regulates hepatic lipid and glucose metabolism. FASEB J. **26:**2209–2221. http://dx.doi.org/10.1096/fj.11-202853.
7. **Kang HW, Ozdemir C, Kawano Y, LeClair KB, Vernochet C, Kahn CR, Hagen SJ, Cohen DE.** 2013. Thioesterase superfamily member 2/acyl-CoA thioesterase 13 (Them2/Acot13) regulates adaptive thermogenesis in mice. J. Biol. Chem. **288:**33376–33386. http://dx.doi.org/10.1074/jbc.M113.481408.
8. **Roderick SL, Chan WW, Agate DS, Olsen LR, Vetting MW, Rajashankar KR, Cohen DE.** 2002. Structure of human phosphatidylcholine transfer protein in complex with its ligand. Nat. Struct. Biol. **9:**507–511. http://dx.doi.org/10.1038/nsb812.
9. **Scapa EF, Pocai A, Wu MK, Gutierrez-Juarez R, Glenz L, Kanno K, Li H, Biddinger S, Jelicks LA, Rossetti L, Cohen DE.** 2008. Regulation of energy substrate utilization and hepatic insulin sensitivity by phosphatidylcholine transfer protein/StarD2. FASEB J. **22:**2579–2590. http://dx.doi.org/10.1096/fj.07-105395.
10. **Ersoy BA, Tarun A, D'Aquino K, Hancer NJ, Ukomadu C, White MF, Michel T, Manning BD, Cohen DE.** 2013. Phosphatidylcholine transfer protein interacts with thioesterase superfamily member 2 to attenuate insulin signaling. Sci. Signal. **6:**ra64. http://dx.doi.org/10.1126/scisignal.2004111.
11. **Kang HW, Kanno K, Scapa EF, Cohen DE.** 2010. Regulatory role for phosphatidylcholine transfer protein/StarD2 in the metabolic response to peroxisome proliferator activated receptor alpha (PPARα). Biochim. Biophys. Acta **1801:**496–502. http://dx.doi.org/10.1016/j.bbalip.2009.12.013.
12. **Kang HW, Wei J, Cohen DE.** 2010. PC-TP/StARD2: of membranes and metabolism. Trends Endocrinol. Metab. **21:**449–456. http://dx.doi.org/10.1016/j.tem.2010.02.001.
13. **Kersten S, Seydoux J, Peters JM, Gonzalez FJ, Desvergne B, Wahli W.** 1999. Peroxisome proliferator-activated receptor alpha mediates the adaptive response to fasting. J. Clin. Invest. **103:**1489–1498. http://dx.doi.org/10.1172/JCI6223.
14. **Lee P, Peng H, Gelbart T, Beutler E.** 2004. The IL-6- and lipopolysaccharide-induced transcription of hepcidin in HFE-, transferrin receptor 2-, and β2-microglobulin-deficient hepatocytes. Proc. Natl. Acad. Sci. U. S. A. **101:**9263–9265. http://dx.doi.org/10.1073/pnas.0403108101.
15. **Ellis JM, Li LO, Wu PC, Koves TR, Ilkayeva O, Stevens RD, Watkins SM, Muoio DM, Coleman RA.** 2010. Adipose acyl-CoA synthetase-1 directs fatty acids toward beta-oxidation and is required for cold thermogenesis. Cell Metab. **12:**53–64. http://dx.doi.org/10.1016/j.cmet.2010.05.012.
16. **Sakai M, Matsumoto M, Tujimura T, Yongheng C, Noguchi T, Inagaki K, Inoue H, Hosooka T, Takazawa K, Kido Y, Yasuda K, Hiramatsu R, Matsuki Y, Kasuga M.** 2012. CITED2 links hormonal signaling to PGC-1α acetylation in the regulation of gluconeogenesis. Nat. Med. **18:**612–617. http://dx.doi.org/10.1038/nm.2691.
17. **Shishova EY, Stoll JM, Ersoy BA, Shrestha S, Scapa EF, Li Y, Niepel MW, Su Y, Jelicks LA, Stahl GL, Glicksman MA, Gutierrez-Juarez R, Cuny GD, Cohen DE.** 2011. Genetic ablation or chemical inhibition of phosphatidylcholine transfer protein attenuates diet-induced hepatic glucose production. Hepatology **54:**664–674. http://dx.doi.org/10.1002/hep.24393.
18. **Lee AH, Scapa EF, Cohen DE, Glimcher LH.** 2008. Regulation of hepatic lipogenesis by the transcription factor XBP1. Science **320:**1492–1496. http://dx.doi.org/10.1126/science.1158042.
19. **Burgess SC, He T, Yan Z, Lindner J, Sherry AD, Malloy CR, Browning JD, Magnuson MA.** 2007. Cytosolic phosphoenolpyruvate carboxykinase does not solely control the rate of hepatic gluconeogenesis in the intact mouse liver. Cell Metab. **5:**313–320. http://dx.doi.org/10.1016/j.cmet.2007.03.004.
20. **Burgess SC, Leone TC, Wende AR, Croce MA, Chen Z, Sherry AD, Malloy CR, Finck BN.** 2006. Diminished hepatic gluconeogenesis via defects in tricarboxylic acid cycle flux in peroxisome proliferator-activated receptor gamma coactivator-1α (PGC-1α)-deficient mice. J. Biol. Chem. **281:**19000–19008. http://dx.doi.org/10.1074/jbc.M600050200.
21. **Chutkow WA, Patwari P, Yoshioka J, Lee RT.** 2008. Thioredoxin-interacting protein (Txnip) is a critical regulator of hepatic glucose production. J. Biol. Chem. **283:**2397–2406. http://dx.doi.org/10.1074/jbc.M708169200.
22. **Foster DW.** 2012. Malonyl-CoA: the regulator of fatty acid synthesis and oxidation. J. Clin. Invest. **122:**1958–1959. http://dx.doi.org/10.1172/JCI63967.
23. **Badman MK, Pissios P, Kennedy AR, Koukos G, Flier JS, Maratos-Flier E.** 2007. Hepatic fibroblast growth factor 21 is regulated by PPARα and is a key mediator of hepatic lipid metabolism in ketotic states. Cell Metab. **5:**426–437. http://dx.doi.org/10.1016/j.cmet.2007.05.002.
24. **Potthoff MJ, Inagaki T, Satapati S, Ding X, He T, Goetz R, Mohammadi M, Finck BN, Mangelsdorf DJ, Kliewer SA, Burgess SC.** 2009. FGF21 induces PGC-1α and regulates carbohydrate and fatty acid metabolism during the adaptive starvation response. Proc. Natl. Acad. Sci. U. S. A. **106:**10853–10858. http://dx.doi.org/10.1073/pnas.0904187106.
25. **Hondares E, Rosell M, Diaz-Delfin J, Olmos Y, Monsalve M, Iglesias R, Villarroya F, Giralt M.** 2011. Peroxisome proliferator-activated receptor alpha (PPARα) induces PPARγ coactivator 1α (PGC-1α) gene expression and contributes to thermogenic activation of brown fat: involvement of PRDM16. J. Biol. Chem. **286:**43112–43122. http://dx.doi.org/10.1074/jbc.M111.252775.
26. **Kawano Y, Cohen DE.** 2013. Mechanisms of hepatic triglyceride accumulation in non-alcoholic fatty liver disease. J. Gastroenterol. **48:**434–441. http://dx.doi.org/10.1007/s00535-013-0758-5.
27. **Wagle N, Xian J, Shishova EY, Wei J, Glicksman MA, Cuny GD, Stein RL, Cohen DE.** 2008. Small-molecule inhibitors of phosphatidylcholine transfer protein/StarD2 identified by high-throughput screening. Anal. Biochem. **383:**85–92. http://dx.doi.org/10.1016/j.ab.2008.07.039.
28. **Lee K, Kerner J, Hoppel CL.** 2011. Mitochondrial carnitine palmitoyltransferase 1a (CPT1a) is part of an outer membrane fatty acid transfer complex. J. Biol. Chem. **286:**25655–25662. http://dx.doi.org/10.1074/jbc.M111.228692.
29. **Kerner J, Hoppel C.** 2000. Fatty acid import into mitochondria. Biochim. Biophys. Acta **1486:**1–17. http://dx.doi.org/10.1016/S1388-1981(00)00044-5.
30. **Rinaldo P, Matern D, Bennett MJ.** 2002. Fatty acid oxidation disorders. Annu. Rev. Physiol. **64:**477–502. http://dx.doi.org/10.1146/annurev.physiol.64.082201.154705.
31. **Longuet C, Sinclair EM, Maida A, Baggio LL, Maziarz M, Charron MJ, Drucker DJ.** 2008. The glucagon receptor is required for the adaptive metabolic response to fasting. Cell Metab. **8:**359–371. http://dx.doi.org/10.1016/j.cmet.2008.09.008.
32. **Owen OE, Kalhan SC, Hanson RW.** 2002. The key role of anaplerosis and cataplerosis for citric acid cycle function. J. Biol. Chem. **277:**30409–30412. http://dx.doi.org/10.1074/jbc.R200006200.
33. **Jenkins CM, Yang J, Sims HF, Gross RW.** 2011. Reversible high affinity inhibition of phosphofructokinase-1 by acyl-CoA: a mechanism integrating glycolytic flux with lipid metabolism. J. Biol. Chem. **286:**11937–11950. http://dx.doi.org/10.1074/jbc.M110.203661.

34. **Wu Z, Puigserver P, Andersson U, Zhang C, Adelmant G, Mootha V, Troy A, Cinti S, Lowell B, Scarpulla RC, Spiegelman BM.** 1999. Mechanisms controlling mitochondrial biogenesis and respiration through the thermogenic coactivator PGC-1. Cell **98:**115–124. http://dx.doi.org/10.1016/S0092-8674(00)80611-X.
35. **Yoon MJ, Lee GY, Chung JJ, Ahn YH, Hong SH, Kim JB.** 2006. Adiponectin increases fatty acid oxidation in skeletal muscle cells by sequential activation of AMP-activated protein kinase, p38 mitogen-activated protein kinase, and peroxisome proliferator-activated receptor alpha. Diabetes **55:**2562–2570. http://dx.doi.org/10.2337/db05-1322.
36. **Foretz M, Ancellin N, Andreelli F, Saintillan Y, Grondin P, Kahn A, Thorens B, Vaulont S, Viollet B.** 2005. Short-term overexpression of a constitutively active form of AMP-activated protein kinase in the liver leads to mild hypoglycemia and fatty liver. Diabetes **54:**1331–1339. http://dx.doi.org/10.2337/diabetes.54.5.1331.
37. **Taylor EB, Ellingson WJ, Lamb JD, Chesser DG, Winder WW.** 2005. Long-chain acyl-CoA esters inhibit phosphorylation of AMP-activated protein kinase at threonine-172 by LKB1/STRAD/MO25. Am. J. Physiol. Endocrinol. Metab. **288:**E1055–E1061. http://dx.doi.org/10.1152/ajpendo.00516.2004.
38. **Guillou H, Martin P, Jan S, D'Andrea S, Roulet A, Catheline D, Rioux V, Pineau T, Legrand P.** 2002. Comparative effect of fenofibrate on hepatic desaturases in wild-type and peroxisome proliferator-activated receptor alpha-deficient mice. Lipids **37:**981–989. http://dx.doi.org/10.1007/s11745-006-0990-3.
39. **Tang C, Cho HP, Nakamura MT, Clarke SD.** 2003. Regulation of human Δ-6 desaturase gene transcription: identification of a functional direct repeat-1 element. J. Lipid Res. **44:**686–695. http://dx.doi.org/10.1194/jlr.M200195-JLR200.
40. **Wheelock CE, Goto S, Hammock BD, Newman JW.** 2007. Clofibrate-induced changes in the liver, heart, brain and white adipose lipid metabolome of Swiss-Webster mice. Metabolomics **3:**137–145. http://dx.doi.org/10.1007/s11306-007-0052-8.